Effect of Pt substitution on the magnetocrystalline anisotropy of Ni_2MnGa: A competition between chemistry and elasticity

L. Caron,[1] B. Dutta,[2] P. Devi,[1] M. Ghorbani Zavareh,[1] T. Hickel,[2] R. Cabassi,[3] F. Bolzoni,[3] S. Fabbrici,[3] F. Albertini,[3] C. Felser,[1] and Sanjay Singh[1,*]

[1]*Max Planck Institute for Chemical Physics of Solids, Nöthnitzer Str. 40, 01187 Dresden, Germany*

[2]*Max-Planck-Institut für Eisenforschung GmbH Max-Planck-Strasse 1, 40237 Düsseldorf, Germany*

[3]*C.N.R.–I.M.E.M. Institute, Parco Area delle Scienze, 37A, 43010 Fontanini–Parma, Italy*

(Received 30 December 2016; revised manuscript received 10 April 2017; published 7 August 2017)

The magnetocrystalline anisotropy (MAE) of $Ni_{2-x}Pt_xMnGa(0 \leqslant x \leqslant 0.25)$ alloys are investigated using the singular point detection technique and density functional theory. A slight reduction in MAE as compared to that of Ni_2MnGa is observed due to Pt substitution. The calculated MAE varies almost linearly with the orbital moment anisotropy. A competition between the elastic and the chemical contributions explains the observed trend of the MAE with increasing Pt content. The large MAE in combination with the previously reported increase of the martensitic transition temperature makes these alloys promising candidates for ferromagnetic shape memory applications near room temperature.

DOI: 10.1103/PhysRevB.96.054105

Large magnetic field induced strain (MFIS) of ferromagnetic shape memory alloys (FSMA's) [1–7], which is an order of magnitude larger than that of magnetostrictive materials, makes these alloys promising materials for designing microactuators. Ni_2MnGa is the most important FSMA that shows MFIS of about 10%, which is comparable to the strain induced by temperature in nonmagnetic shape memory alloys [1,2]. Ni_2MnGa shows a structural phase transition from high-temperature cubic austenite (high symmetry) to low-temperature martensite (lower symmetry) at around 210 K and a purely magnetic transition from paramagnetic to ferromagnetic at 370 K [8,9]. The structural transformation in Ni_2MnGa is a displacive transition, where a large number of differently aligned twin variants are generated in the martensite phase. Due to the high magnetocrystalline anisotropy, these twin variants may be rearranged by the application of an external magnetic field, giving rise to large strains [2,10].

Although Ni_2MnGa shows the large MFIS, its practical application is hindered by a low martensitic transformation temperature (T_M) and poor mechanical stability. To overcome these limitations, different strategies have been adopted over the years with appropriate doping proving to be the most successful route to tune and achieve the desired material properties [11]. The advancements made with such an approach can be highlighted for Heusler alloys such as Ni-Mn-Fe-Ga [12], Ni-Fe-Ga-Co [13], and Ni-Mn-Co-Ga [14], which show improved ductile behavior. However, the MFIS in these alloys is much smaller than that of Ni_2MnGa which makes them ill suited for real applications.

In recent studies, Pt substituted Ni_2MnGa alloys have emerged as promising materials for practical applications due to a higher T_M value [15] and better mechanical properties [16]. Our theoretical studies provided insights into the chemical trends for martensitic transformations in $Ni_{2-x}Pt_xMnGa$ [17,18]. The free energies obtained by combining density functional theory (DFT) with thermodynamic concepts for all excitation processes contributing to the entropy indicated that the martensitic transformation in these alloys follows the same mechanisms as in the case of Ni_2MnGa [19,20]. The delicate interplay between the magnetic and the vibrational degrees of freedom determine the actual transformation temperature. Recently, we have measured the experimental phase diagram [21] of $Ni_{2-x}Pt_xMnGa$ and the obtained results are in a very good agreement with theoretical predictions [17,18]. The T_M shows an increasing trend with increasing Pt content up to $Ni_{1.6}Pt_{0.4}MnGa$, above which the Curie temperature (T_C) and T_M coincide.

For the impact of Pt on the MFIS in $Ni_{2-x}Pt_xMnGa$, however, such clear indications are lacking in recent investigations. The observation of a 7M orthorhombic modulated structure in the martensite phase and a change in sign of the magnetocaloric effect (inverse to conventional) in $Ni_{1.8}Pt_{0.2}MnGa$ [22,23] suggest that the same features which give rise to MFIS in Ni_2MnGa [24–26] are also present in the Pt-substituted alloys and hence a large MFIS can be expected in $Ni_{2-x}Pt_xMnGa$ as well. Such an expectation is supported by the prediction of Siewert *et al.* [17], who used *ab initio* calculations to estimate the maximum achievable strain in this system to be around 14% [17]. These findings augur well for the longstanding search of FSMA's for high temperature applications. While a direct evidence of a large MFIS in these systems is still missing, the magnetic anisotropy can provide information on the MFIS in these alloys, since it is the driving force for the rearrangement of martensitic variants under applied magnetic field.

In the present work we investigate the MAE in the martensite phase of $Ni_{2-x}Pt_xMnGa$ ($0 \leqslant x \leqslant 0.25$) FSMA's. The spin-orbit coupling in $3d$ transition metals is usually weak which translates into their small MAE value. The substitution of Pt which is a $5d$ element with almost an order of magnitude larger spin-orbit coupling parameter than Ni is expected to increase the MAE in $Ni_{2-x}Pt_xMnGa$. Contrary to our expectations, the experimental measurements reveal a slight decrease in the MAE with increasing Pt content for the $Ni_{2-x}Pt_xMnGa$ alloys. Our theoretical analysis indicates that the observed changes in MAE result from a competition between a chemical

*sanjay.singh@cpfs.mpg.de; present address: School of Materials Science and Technology, Indian Institute of Technology (BHU) Varanasi-221005, India.

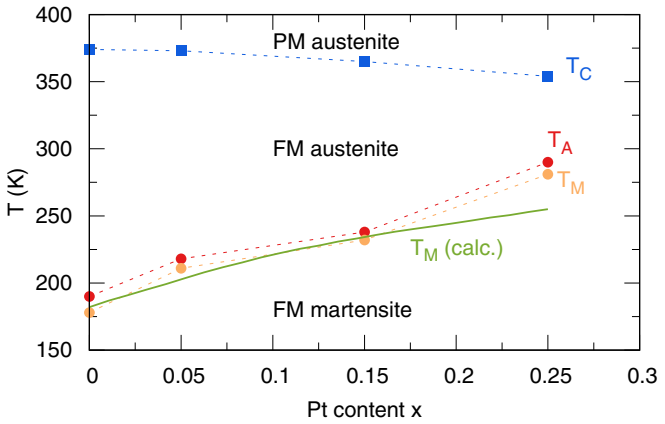

FIG. 1. Martensitic start (T_M), austenitic start (T_A), and magnetic transition temperature (T_C) of $Ni_{2-x}Pt_xMnGa$ as a function of chemical composition x as obtained in our measurements. Our previous theoretical results on T_M [18] are also shown for comparison.

effect due to change in the alloy composition (chemistry) and an elastic effect due to change in the structural parameters (elasticity).

In Fig. 1 we present a summary of structural and magnetic transitions in $Ni_{2-x}Pt_xMnGa$ ($x = 0, 0.05, 0.15, 0.25$) samples used in the present study (see Supplemental Material [27]). The variation of the measured transition temperatures is in very good agreement with our calculations [18]. The small difference in magnitude between the measured and the calculated values can be attributed to the fact that in theory only the transformation between austenite and nonmodulated martensite was considered while, in experiments [22,41], a 7M modulated martensite structure is, for example, observed for $x = 0.1$ and 0.25. Contrary to T_M, the T_C in $Ni_{2-x}Pt_xMnGa$ decreases linearly with increasing Pt content.

To investigate the magnetocrystalline anisotropy experimentally, the singular point detection (SPD) [42,43] technique is used. Magnetization measurements under pulsed magnetic fields are performed on powder samples oriented by a rotating magnetic field in the plane perpendicular to the applied magnetic field used for the pulsed field measurements. Since the residual stresses generated during grinding the ingot into powder may stabilize the martensite phase even above the T_M [44,45], the powder samples were annealed prior to the magnetocrystalline anisotropy measurements. The measurements were carried out while heating the samples from liquid nitrogen (LN_2) temperature (77 K) upon the application of a magnetic field pulse with peak value of 7 T and a rising time of 0.5 ms (see the upper panel of Fig. 2), allowing good field penetration into the samples.

According to SPD, the anisotropy field (H_A) in magnets having an easy axis of magnetization can be evaluated as the position of the peak appearing in the second order derivative of magnetization d^2M/dH^2. This can be done both on the rising and on the descending branch of the magnetic pulse $H(t)$ of Fig. 2 (upper panel) and each one of the two choices has pros and cons. On the rising branch the sweep rate is higher, yielding a stronger measured signal: this provides better sensitivity when measuring, for instance, small amounts of material or poorly oriented samples. On the other hand, high sweep rates

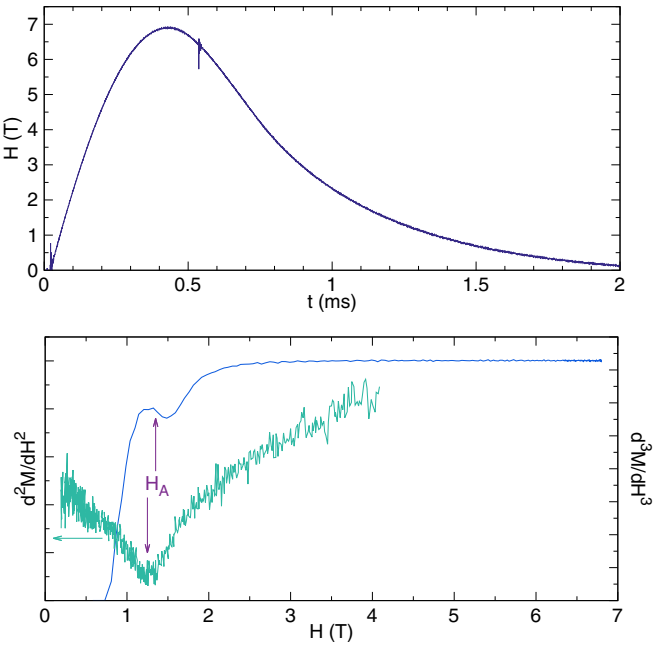

FIG. 2. Example of singular point detection measurement for $Ni_{1.85}Pt_{0.15}MnGa$ at 213 K. Upper panel: magnetic field pulse. Lower panel: second and third derivatives of the magnetization showing the flexus in d^3M/dH^3 in the increasing $H(t)$ branch and the minimum at d^2M/dH^2 in the decreasing $H(t)$ branch.

can induce shielding eddy currents inside the sample: this corresponds to an inaccurate H_A determination because the internal field is lower than the applied field [46]. On the contrary, on the descending branch the sweep rate is lower; therefore, the measured signal is weaker and more noisy, but the position of the SPD peak is closer to the real H_A value. We have measured H_A on both $H(t)$ branches obtaining a good agreement between the two values, which can be considered as a check of the results reliability. We have also measured the third order derivative of the magnetization d^3M/dH^3, whose flexus sometimes provides a more convenient way to read the position of the SPD peak. As an example, in Fig. 2 the measurements for $Ni_{1.85}Pt_{0.15}MnGa$ at $T = 213$ K are shown. H_A is then corrected for demagnetizing factor and, from these, the values of the anisotropy constant $(K_A) = H_A(T)M_S(T)/2$ have been calculated using the saturation magnetization (M_S) values for a given temperature from the isofield magnetization data at 5 T (see Supplemental Material [27]). The cell volume at 300 K have been used to convert M_S in emu/cm^3.

The temperature dependent H_A and K_A for all four samples are shown in Fig. 3(a). The martensite to austenite transition temperatures (T_A) during heating as shown in Fig. 1 are also indicated by vertical lines for all samples. In all cases a singularity in d^2M/dH^2 and d^3M/dH^3 could only be observed at temperatures below T_A, i.e., within the martensite phase. For all samples H_A and K_A are decreasing with increasing temperature up to T_A. The comparison of composition dependent values of H_A and K_A at 78 K is shown in Fig. 3(b). The values of H_A and K_A for the Ni_2MnGa sample used here are in good agreement with results reported in the literature [47,48]. From comparison it is clear that with

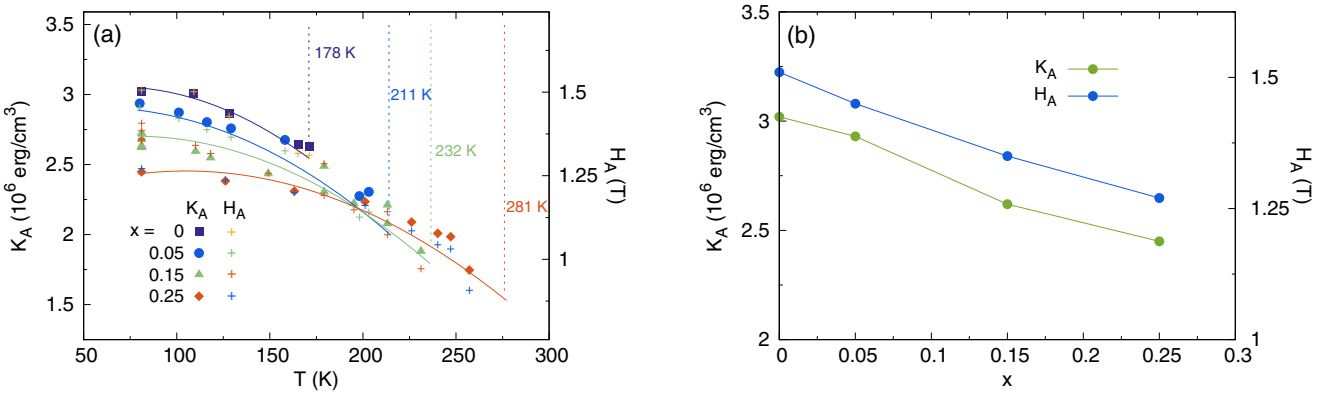

FIG. 3. (a) Anisotropy constant (K_A) and anisotropy field (H_A) as a function of temperature for polycrystalline $Ni_{2-x}Pt_xMnGa$ ($0 \leqslant x \leqslant 0.25$) alloys. The vertical dashed lines correspond to the temperatures where the martensite to austenite transition starts on heating. Solid lines are guides to the eye used to show the variation. (b) K_A and H_A at 78 K for all measured samples.

replacing Ni by Pt in Ni_2MnGa a nominal decrease of both H_A and K_A is observed. For example, the value of K_A at 78 K decreased from 3.02×10^6 erg/cm^3 for Ni_2MnGa to 2.45×10^6 erg/cm^3 for $Ni_{1.75}Pt_{0.25}MnGa$. This experimental result is indeed promising as the K_A values for all samples studied here are close to that of Ni_2MnGa. However, since the decreasing trend of the MAE with increasing Pt content is in contrast to our expectations, we have performed further theoretical calculations to understand the origin of this trend.

Table I shows the lattice parameters for different Pt concentrations obtained with our *ab initio* calculations (see Supplemental Material [27]). The equilibrium structure of the cubic austenite phase is determined by relaxing all the degrees of freedom in our supercell. Since modulations are expected to have a limited impact on the chemical trend of MAE, theoretical calculations for the martensite phase are mainly performed for the simpler nonmodulated tetragonal structure. As the volume change during martensitic transformation in these alloys is almost negligible [49], we keep the volume for each composition fixed to that of the austenite phase and vary only the *c/a* ratio. As expected, our calculations reveal a volume expansion as well as an increased *c/a* ratio for the martensite phase with increasing Pt content in Ni_2MnGa due to the large atomic size of Pt. Hence substitution of Pt for Ni not only changes the electronic structure (chemistry) but also the structural properties (elasticity), which can be significant for the MAE.

We next calculate the MAE and orbital moments for the nonmodulated martensite phase. Both MAE and orbital moments are relativistic effects that require well-converged wave functions and charge densities [50,51]. To achieve this a stringent convergence criteria of 10^{-8} eV for the electronic structure is used. An increased energy cutoff of 500 eV and a denser k-point grid of $6 \times 6 \times 6$ which resulted in 216 inequivalent k points in the Brillouin zone are also chosen. The calculations for the MAE have been performed in two steps. In the first step, the charge densities and the wave functions are determined for the previously relaxed structures with improved cutoff parameters from self-consistent scalar-relativistic calculations. Then, in a second step, the converged charge densities and the wave functions are used for the relativistic calculations with spin-orbit coupling to compute the total energies for different directions of spin polarizations. The MAE is calculated from the difference of the total energies between easy and hard axes. Due to the small energy difference ($\sim 0.1 \times 10^6$ erg/cm^3) between the two formally equivalent directions ([100] and [010] in the nonmodulated martensite) caused by the disordered configurations, we average the energies for these two directions of spin polarizations.

TABLE I. Calculated lattice parameters for $Ni_{2-x}Pt_xMnGa$ ($0 \leqslant x \leqslant 0.25$).

Pt content	Lattice parameters (Å) Austenite $a = b = c$	Nonmodulated $a = b$	Martensite c/a
0	5.801	5.378	1.255
0.031	5.809	5.379	1.259
0.125	5.835	5.397	1.263
0.250	5.868	5.410	1.276

Our calculated results show that the MAE decreases monotonically with increasing Pt content (Fig. 4), which is in agreement with the experimental observation (Fig. 4, inset). The orbital moment anisotropy (OMA) obtained from the difference in the orbital moments between the easy axis and the hard axis alignment of the magnetization shows a similar trend as the MAE. This suggests a direct relation between the MAE and the OMA similar to what has been investigated in a wide variety of other systems [52–55]. It should be noted here that while the trends for the MAE and the K_A as obtained from theory and experiment respectively match very well, their absolute values still differ significantly for all compositions. Such a difference in the MAE can originate from the choice of the structural model. In our theoretical calculations we have considered a nonmodulated tetragonal martensite structure with $c/a > 1$, while the samples used in experiment have predominantly a modulated martensite structure with $c/a < 1$ [19].

To gain insight into the impact of tetragonality and structural modulation on the MAE, we next calculate the MAE for nonmodulated Ni_2MnGa as a function of the c/a ratio. The obtained results [Fig. 5(a)] indicate that the MAE

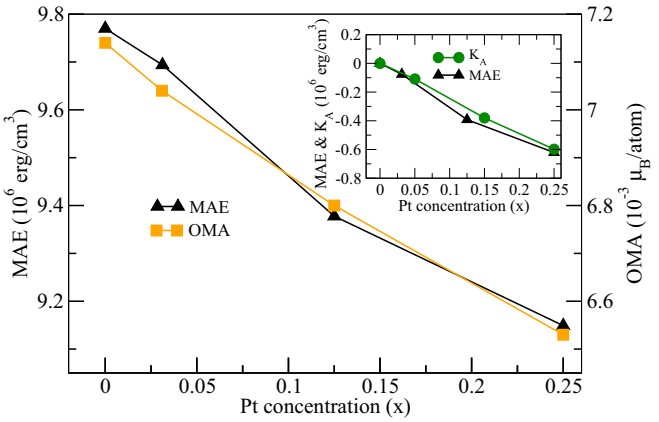

FIG. 4. Dependence of the MAE and the OMA on the Pt concentration in $Ni_{2-x}Pt_xMnGa$ as obtained from *ab initio* calculations. The inset shows the variation of the theoretically calculated MAE and the experimentally determined K_A with increasing Pt concentration. Both quantities in the inset are plotted taking their respective values for Ni_2MnGa as a reference.

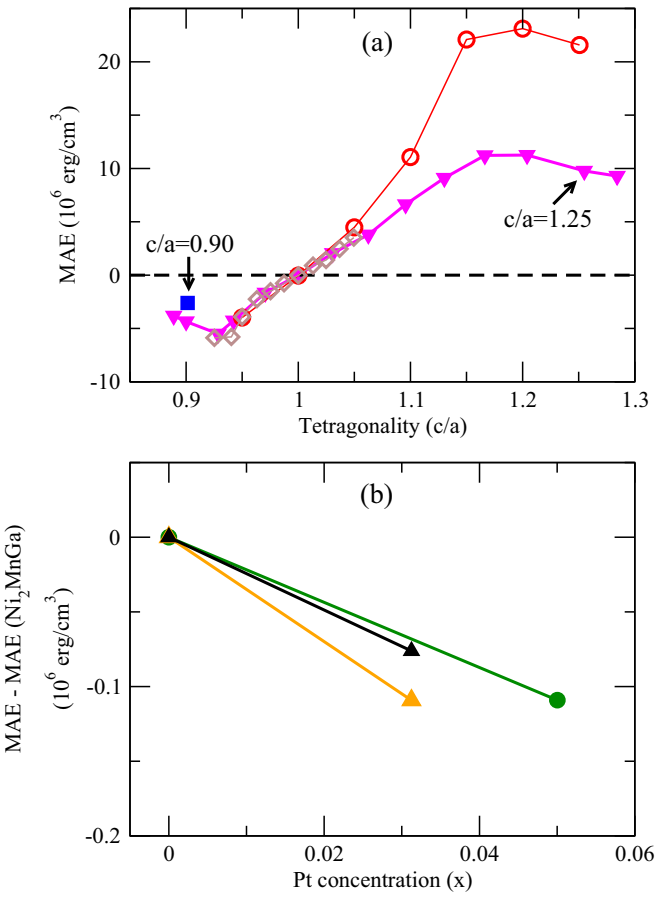

FIG. 5. (a) Calculated MAE of nonmodulated Ni_2MnGa for different c/a ratios. Magenta ▼ indicate results obtained by us, while ◇ and ○ symbols refer to previous theoretical results published in Refs. [56,57], respectively. The MAE for the $7M$ martensite phase is marked by ■. (b) Calculated MAE as a function of the Pt concentration in $Ni_{2-x}Pt_xMnGa$ for nonmodulated tetragonal structures with $c/a \approx 1.25$ (▲) and 0.90 (▲). ● correspond to experimental data. All MAEs are plotted taking the MAE of Ni_2MnGa as the reference.

depends sensitively on the tetragonality of the lattice. We find an easy plane MAE for $c/a > 1$, while for $c/a < 1$ the c axis is the easy direction. Our calculations in general show a good agreement with previous theoretical results [56,57]. For $c/a \geqslant 1$, Gruner *et al.* [57] found a higher MAE as compared to our calculated values which might be due to the different *ab initio* methods (different basis set and exchange-correlation functional) employed in the two sets of calculations. In the next step, we calculate the MAE for the $7M$ martensite phase of Ni_2MnGa. This modulated structure has $c/a \approx 0.90$ within our nomenclature, though approaches deriving it from the concept of adaptive martensite [10] occasionally discuss it using nonmodulated martensite building blocks with $c/a = 1.25$. For this calculation, a $7 \times 1 \times 1$ unit cell (56 atoms) with a k-point grid of $3 \times 21 \times 9$ and an energy cutoff of 500 eV is used. Such a combination of unit cell and k-point grid ensures almost the same value for the quantity "number of atoms × number of k points" for the nonmodulated and the $7M$ martensites [58]. Our calculations reveal [Fig. 5(a)] an uniaxial anisotropy for the $7M$ martensite with the shortest c axis ([001] direction) being the preferred direction for the alignment of the magnetization. Due to the orthorhombic crystal structure, the two hard magnetization axes of the $7M$ martensite have slightly different MAE values [-2.84×10^6 erg/cm^3 for [100] direction (hard axis) and -2.37×10^6 erg/cm^3 for [010] direction (midhard axis)]. This observation, which is in agreement with a previous experimental result [59], indicates that the MAEs for different martensitic phases reported in the literature for Ni_2MnGa do not have a common easy axis: while the nonmodulated tetragonal martensite ($c/a \approx 1.25$) has an easy plane MAE, the modulated $7M$ ($c/a \approx 0.90$) martensite has an easy axis MAE. Figure 5(a) also shows that the absolute values of the MAE for different martensites should be substantially different, with the nonmodulated martensite having an MAE that is almost three times higher than that of the $7M$ phase. The good agreement between the absolute values of our calculated and measured (3.03×10^6 erg/cm^3) MAE and those obtained previously with a phenomenological model [10] ($K_a = 1.63 \times 10^6$ erg/cm^3; $K_b = 0.65 \times 10^6$ erg/cm^3) for the $7M$ martensite of stoichiometric Ni_2MnGa further suggests that the shift required in Fig. 4 is due to the choice of the nonmodulated martensite in theoretical calculations. It should also be noted that structural twinning arrangement or modulation has little impact on the MAE as the nonmodulated structure with $c/a \approx 0.90$ and the $7M$ martensite have almost similar MAE values.

While the MAE for the $7M$ martensite of Ni_2MnGa has been calculated with reasonable computational effort, a determination of the Pt-concentration dependent MAE for this phase is extremely demanding. Already the lowest concentration of Pt in the $7M$ martensite (1 out of 56 atoms) requires an optimization of the crystal structures for several positions of the Pt atom with respect to the twin boundary and a subsequent computation of the MAE for each of them. Additional complexities will arise in a situation with multiple Pt atoms which is required for the full Pt-concentration dependent study of the MAE. Considering the high numerical precision required for a reliable estimation of the MAE, the above calculations will require large conputational time, which is beyond the scope of the present work. Nevertheless,

the chemical trends for the MAE in $Ni_{2-x}Pt_xMnGa$ and the main conclusions derived from our theoretical calculations for the nonmodulated martensite should remain unchanged even for the $7M$ martensite. To validate this statement, we have calculated the MAE for $Ni_{2-x}Pt_xMnGa$ at $x \approx 0.03$ for the nonmodulated structure with a c/a ratio ($\approx$0.90) similar to that of the $7M$ martensite [Fig. 5(b)]. It can be clearly seen that the MAE shows a decreasing trend with increasing Pt content, which matches well with the experimental observations and the theoretical results for nonmodulated martensite with $c/a \approx 1.25$. Since the MAE values do not depend significantly on the structural twinning, it can be expected that the MAE values for the $7M$ martensite will change similarly with Pt substitution.

Next, we investigate the origin of the chemical trend for the MAE in $Ni_{2-x}Pt_xMnGa$, which requires a separation of the chemical contribution from the structural or elastic changes caused by the substitution of Pt for Ni in Ni_2MnGa. While the impact of the chemical doping alone is estimated by calculating the MAE for each composition at the optimized lattice geometry of Ni_2MnGa, the sole contribution resulting from the changes in the elastic effect is determined from the MAE values calculated for Ni_2MnGa at the relaxed structures obtained with different Pt contents. The obtained results presented in Fig. 6 show that the chemical and the structural changes due to Pt substitution influence the MAE in an opposite way. Due to the larger orbital moment of Pt, the MAE resulting from the chemical effect increases monotonically [Fig. 6(a)] with increasing Pt content. Contrary to this, the increase in *c/a* ratio due to Pt substitution leads to a relatively sharp decrease in the MAE, while the internal ionic relaxations due to the size difference of Ni and Pt atoms change the results only slightly [Fig. 6(b)]. This indicates that the changes in the MAE for $Ni_{2-x}Pt_xMnGa$ as obtained in our calculations result from the interplay of these two contributions. The increase in the MAE due to chemical effect is compensated by the dominant elastic effect, which determines the resulting composition-dependent changes in the MAE for these alloys.

To summarize, we have studied the magnetocrystalline anisotropy in $Ni_{2-x}Pt_xMnGa$ ($0 \leqslant x \leqslant 0.25$) alloys. In contrast to the general expectation, our experimental measurements revealed a slight reduction in the MAE due to Pt substitution in Ni_2MnGa, which is correctly captured by DFT simulations. Our theoretical calculations suggest that all the necessary insights on the observed chemical trends for the MAE of $Ni_{2-x}Pt_xMnGa$ can be obtained from the simpler nonmodulated martensite. A better quantitative agreement between the theoretically calculated and the experimentally determined MAE is however achieved for Ni_2MnGa on considering $7M$ modulated martensite in theoretical calculations. We also find that the observed trend for MAE in $Ni_{2-x}Pt_xMnGa$ is a result of the interplay between elastic (structural changes) and chemical (compositional changes) effects, which contribute in an opposite way to the overall MAE. The large MAEs and high martensitic transition temperatures make these alloys ideal candidates for magnetic actuators. The physical insights on the MAE achieved in the present study will be helpful to design new FSMA's in the future.

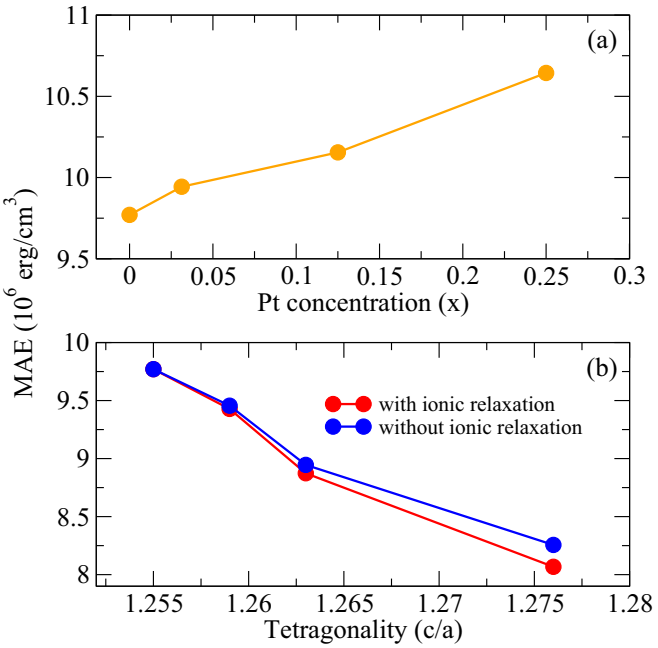

FIG. 6. Changes in the MAE resulting from (a) the chemical effect and (b) the elastic effect due to different Pt concentrations. Ionic relaxation refers to optimization of internal coordinates.

The work was financially supported by the ERC AG No. 291472 "IDEA Heusler!". B.D. and T.H. gratefully acknowledge Deutsche Forschungsgemeinschaft (Germany) for their funding within the priority program SPP1599. S.S. thanks the Alexander von Humboldt foundation for fellowship support.

[1] K. Ullakko, J. K. Huang, C. Kantner, R. C. O'Handley, and V. V. Kokorin, Appl. Phys. Lett. **69**, 1966 (1996).
[2] A. Sozinov, A. A. Likhachev, N. Lanska, and K. Ullakko, Appl. Phys. Lett. **80**, 1746 (2002).
[3] S. J. Murray, M. Marioni, S. M. Allen, R. C. OHandley, and T. A. Lograsso, Appl. Phys. Lett. **77**, 886 (2000).
[4] M. Chmielus, X. X. Zhang, C. Witherspoon, D. C. Dunand, and P. Müllner, Nat. Mater. **8**, 863 (2009).
[5] J. A. Monroe, I. Karaman, B. Basaran, W. Ito, R. Y. Umetsu, R. Kainuma, K. Koyama, and Y. I. Chumlyakov, Acta Mater. **60**, 6883 (2012).
[6] A. Sozinov, N. Lanska, A. Soroka, and W. Zou, Appl. Phys. Lett. **102**, 021902 (2013).
[7] *Shape Memory Alloys*, edited by D. C. Lagoudas (Springer Science+Business Media, LLC, New York, 2008).
[8] S. Singh, J. Nayak, A. Rai, P. Rajput, A. H. Hill, S. R. Barman, and D. Pandey, J. Phys.: Condens. Matter **25**, 212203 (2013).

[9] P. J. Webster, K. R. A. Ziebeck, S. L. Town, and M. S. Peak, Philos. Mag. B **49**, 295 (1984).

[10] S. Kaufmann, U. K. Rößler, O. Heczko, M. Wuttig, J. Buschbeck, L. Schultz, and S. Fähler, Phys. Rev. Lett. **104**, 145702 (2010).

[11] J. Pons, E. Cesari, C. Seguí, F. Masdeu, and R. Santamarta, Mater. Sci. Eng., A **481-482**, 57 (2008).

[12] K. Koho, O. Soderberg, N. Lanska, Y. Ge, X. Liu, L. Straka, J. Vimpari, O. Heczko, and V. K. Lindroos, Mater. Sci. Eng., A **378**, 384 (2004).

[13] H. Morito, K. Oikawa, A. Fujita, K. Fukamichi, R. Kainuma, and K. Ishida, Scr. Mater. **53**, 1237 (2005).

[14] Y. Ma, S. Yang, Y. Liu, and X. Liu, Acta Mater. **57**, 3232 (2009).

[15] Y. Kishi, Z. Yajima, K. Shimizu, and M. Wuttig, Mater. Sci. Eng., A **378**, 361 (2004).

[16] T. Roy, M. E. Gruner, P. Entel, and A. Chakrabarti, J. Alloys Compd. **632**, 822 (2015).

[17] M. Siewert, M. E. Gruner, A. Dannenberg, A. Chakrabarti, H. C. Herper, M. Wuttig, S. R. Barman, S. Singh, A. Al-Zubi, T. Hickel, J. Neugebauer, M. Gillessen, R. Dronskowski, and P. Entel, Appl. Phys. Lett. **99**, 191904 (2011).

[18] B. Dutta, T. Hickel, P. Entel, and J. Neugebauer, J. Phase Equilib. Diff. **35**, 695 (2014).

[19] B. Dutta, A. Çakır, C. Giacobbe, A. Al-Zubi, T. Hickel, M. Acet, and J. Neugebauer, Phys. Rev. Lett. **116**, 025503 (2016).

[20] M. A. Uijttewaal, T. Hickel, J. Neugebauer, M. E. Gruner, and P. Entel, Phys. Rev. Lett. **102**, 035702 (2009).

[21] S. Singh, S. W. D'Souza, J. Nayak, L. Caron, E. Suard, S. Chadov, and C. Felser, Phys. Rev. B **93**, 134102 (2016).

[22] S. Singh, K. R. A. Ziebeck, E. Suard, P. Rajput, S. Bhardwaj, A. M. Awasthi, and S. R. Barman, Appl. Phys. Lett. **101**, 171904 (2012).

[23] S. Singh, S. W. D'Souza, K. Mukherjee, P. Kushwaha, S. R. Barman, S. Agarwal, P. K. Mukhopadhyay, A. Chakrabarti, and E. V. Sampathkumaran, Appl. Phys. Lett. **104**, 231909 (2014).

[24] S. Singh, V. Petricek, P. Rajput, A. H. Hill, E. Suard, S. R. Barman, and D. Pandey, Phys. Rev. B **90**, 014109 (2014).

[25] F. X. Hu, B. G. Shen, J. R. Sun, and G.-H. Wu, Phys. Rev. B **64**, 132412 (2001).

[26] A. Planes, L. Ma nosa, and M. Acet, J. Phys.: Condens. Matter **21**, 233201 (2009).

[27] See Supplemental Material at http://link.aps.org/supplemental/10.1103/PhysRevB.96.054105 for details of sample preparation, measurements, characterizations, and theoretical methods, which includes Refs. [28–40].

[28] A. Zunger, S.-H. Wei, L. G. Ferreira, and J. E. Bernard, Phys. Rev. Lett. **65**, 353 (1990).

[29] A. van de Walle and G. Ceder, J. Phase Equilib. **23**, 348 (2002).

[30] J. Pezold, A. Dick, M. Friak, and J. Neugebauer, Phys. Rev. B **81**, 094203 (2010).

[31] G. Kresse and J. Hafner, Phys. Rev. B **47**, 558(R) (1993).

[32] G. Kresse and J. Furthmller, Phys. Rev. B **54**, 11169 (1996).

[33] P. E. Blöchl, Phys. Rev. B **50**, 17953 (1994).

[34] J. P. Perdew, K. Burke, and M. Ernzerhof, Phys. Rev. Lett. **77**, 3865 (1996).

[35] S. Banik, R. Ranjan, A. Chakrabarti, S. Bhardwaj, N. P. Lalla, A. M. Awasthi, V. Sathe, D. M. Phase, P. K. Mukhopadhyay, D. Pandey, and S. R. Barman, Phys. Rev. B **75**, 104107 (2007).

[36] R. Ranjan, S. Banik, S. R. Barman, U. Kumar, P. K. Mukhopadhyay, and D. Pandey, Phys. Rev. B **74**, 224443 (2006).

[37] S. Singh, S. R. Barman, and D. Pandey, Z. Kristallogr. **230**, 13 (2015).

[38] S. Banik, A. Chakrabarti, U. Kumar, P. K. Mukhopadhyay, A. M. Awasthi, R. Ranjan, J. Schneider, B. L. Ahuja, and S. R. Barman, Phys. Rev. B **74**, 085110 (2006).

[39] A. N. VasilÓv, A. D. Bozhko, V. V. Khovailo, I. E. Dikshtein, V. G. Shavrov, V. D. Buchelnikov, M. Matsumoto, S. Suzuki, T. Takagi, and J. Tani, Phys. Rev. B **59**, 1113 (1999).

[40] K. Ullakko, Y. Ezer, A. Sozinov, G. Kimmel, P. Yakovenko, and V. K. Lindroos, Scr. Mater. **44**, 475 (2001).

[41] S. Singh, B. Dutta, S. W. D'Souza, M. G. Zavareh, P. Devi, A. S. Gibbs, T. Hickel, S. Chadhov, C. Felser, and D. Pandey, arXiv:1611.07538v2.

[42] F. Bolzoni and R. Cabassi, Physica B **346-347**, 524 (2004).

[43] G. Asti and S. Rinaldi, Phys. Rev. Lett. **28**, 1584 (1972).

[44] S. Singh, M. Maniraj, S. W. D'Souza, R. Ranjan, and S. R. Barman, Appl. Phys. Lett. **96**, 081904 (2010).

[45] S. Singh, P. Kushwaha, F. Scheibel, H.-P. Liermann, S. R. Barman, M. Acet, C. Felser, and D. Pandey, Phys. Rev. B **92**, 020105(R) (2015).

[46] F. Bolzoni, Meas. Sci. Technol. **6**, 1186 (1995).

[47] F. Albertini, L. Pareti, A. Paoluzi, L. Morellon, P. A. Algarabel, M. R. Ibarra, and L. Righi, Appl. Phys. Lett. **81**, 4032 (2002).

[48] F. Albertini1, M. Solzi, A. Paoluzi, and L. Righi, Mater. Sci. Forum **583**, 169 (2008).

[49] P. I. Polyakov, V. V. Slyusarev, V. V. Kokorin, S. M. Konoplyuk, Y. S. Semenova, and V. V. Khovaylo, J. Mater. Eng. Perform. **23**, 3180 (2014).

[50] A. Lehnert, S. Dennler, P. Błoński, S. Rusponi, M. Etzkorn, G. Moulas, P. Bencok, P. Gambardella, H. Brune, and J. Hafner, Phys. Rev. B **82**, 094409 (2010).

[51] C. Antoniak, M. E. Gruner, M. Spasova, A. V. Trunova, F. M. Römer, A. Warland, B. Krumme, K. Fauth, S. Sun, P. Entel, M. Farle, and H. Wende, Nat. Commun. **2**, 528 (2011).

[52] P. Bruno, Phys. Rev. B **39**, 865 (1989).

[53] G. H. O. Daalderop, P. J. Kelly, and M. F. H. Schuurmans, Phys. Rev. B **44**, 12054 (1991).

[54] C. Andersson, B. Sanyal, O. Eriksson, L. Nordström, O. Karis, D. Arvanitis, T. Konishi, E. Holub-Krappe, and J. H. Dunn, Phys. Rev. Lett. **99**, 177207 (2007).

[55] M. M. Soares, A. D. Lamirand, A. Y. Ramos, M. De Santis, and H. C. N. Tolentino, Phys. Rev. B **90**, 214403 (2014).

[56] J. Enkovaara, A. Ayuela, L. Nordström, and R. M. Nieminen, Phys. Rev. B **65**, 134422 (2002).

[57] M. Gruner, P. Entel, I. Opahle, and M. Richter, J. Mater. Sci. **43**, 3825 (2008).

[58] B. Grabowski, T. Hickel, and J. Neugebauer, Phys. Rev. B **76**, 024309 (2007).

[59] L. Straka and O. Heczko, J. Appl. Phys. **93**, 8636 (2003).